Title

NADPH Oxidase Contributes to Photoreceptor Degeneration in Constitutively Active RAC1 MiceNADPH Oxidase in RAC1-Induced Rod Degeneration

Journal

Investigative Ophthalmology & Visual Science, 57(6)

ISSN

0146-0404

Authors

Song, Hongman
Vijayasarathy, Camasamudram
Zeng, Yong
et al.

Publication Date

2016-05-27

DOI

10.1167/iovs.15-18974

Peer reviewed

NADPH Oxidase Contributes to Photoreceptor Degeneration in Constitutively Active RAC1 Mice

Hongman Song,[1] Camasamudram Vijayasarathy,[1] Yong Zeng,[1] Dario Marangoni,[1] Ronald A. Bush,[1] Zhijian Wu,[2] and Paul A. Sieving[1,3]

[1]Section for Translational Research on Retinal and Macular Degeneration, National Institute on Deafness and Other Communication Disorders, National Institutes of Health, Bethesda, Maryland, United States
[2]Ocular Gene Therapy Core, National Eye Institute, National Institutes of Health, Bethesda, Maryland, United States
[3]National Eye Institute, National Institutes of Health, Bethesda, Maryland, United States

Correspondence: Paul A. Sieving, BG 31, RM6A03, 31 Center Drive, Bethesda, MD 20892, USA; paulsieving@nei.nih.gov.

Submitted: December 17, 2015
Accepted: April 11, 2016

Citation: Song H, Vijayasarathy C, Zeng Y, et al. NADPH oxidase contributes to photoreceptor degeneration in constitutively active RAC1 mice. *Invest Ophthalmol Vis Sci.* 2016;57:2864–2875. DOI:10.1167/iovs.15-18974

Purpose. The active form of small GTPase RAC1 is required for activation of NADPH oxidase (NOX), which in turn generates reactive oxygen species (ROS) in nonphagocytic cells. We explored whether NOX-induced oxidative stress contributes to rod degeneration in retinas expressing constitutively active (CA) RAC1.

Methods. Transgenic (Tg)–CA-RAC1 mice were given apocynin (10 mg/kg, intraperitoneal), a NOX inhibitor, or vehicle daily for up to 13 weeks. Superoxide production and oxidative damage were assessed by dihydroethidium staining and by protein carbonyls and malondialdehyde levels, respectively. Outer nuclear layer (ONL) cells were counted and electroretinogram (ERG) amplitudes measured in Tg-CA-RAC1 mice. Outer nuclear layer cells were counted in wild-type (WT) mice after transfer of *CA-Rac1* gene by subretinal injection of AAV8-*pOpsin-CA Rac1-GFP*.

Results. Transgenic-CA-RAC1 retinas had significantly fewer photoreceptor cells and more apoptotic ONL cells than WT controls from postnatal week (Pw) 3 to Pw13. Superoxide accumulation and protein and lipid oxidation were increased in Tg-CA-RAC1 retinas and were reduced in mice treated with apocynin. Apocynin reduced the loss of photoreceptors and increased the rod ERG a- and b-wave amplitudes when compared with vehicle-injected transgenic controls. Photoreceptor loss was also observed in regions of adult WT retina transduced with AAV8-*pOpsin-CA Rac1-GFP* but not in neighboring regions that were not transduced or in AAV8-*pOpsin-GFP*–transduced retinas.

Conclusions. Constitutively active RAC1 promotes photoreceptor cell death by oxidative damage that occurs, at least partially, through NOX-induced ROS. Reactive oxygen species are likely involved in multiple forms of retinal degenerations, and our results support investigating RAC1 inhibition as a therapeutic approach that targets this disease pathway.

Keywords: photoreceptor degeneration, RAC1, NADPH oxidase, reactive oxygen species, oxidative stress

Retinal degenerations can be triggered by genetic mutations or by excessive light exposure. The common feature of such disorders is apoptosis of photoreceptor cells.[1–6] Photoreceptors have high oxygen consumption,[7,8] high amounts of polyunsaturated fatty acids,[9–11] and high metabolic activity[4] but low levels of antioxidants in the outer segments,[12] which render them at high risk for oxidative damage. Oxidative stress is induced through the excessive generation of reactive oxygen species (ROS), including superoxide, hydrogen peroxide, hydroxyl radicals, and peroxynitrite, that can modify and damage cellular lipids, proteins, and DNA.[13] Thus, increased oxidative stress disturbs the normal redox homeostasis, resulting in toxicity and cell death,[14] and contributes to the progression of neurodegenerative diseases.[13,15]

There is increasing evidence that ROS and oxidative stress play a critical role in the pathogenesis of many retinal degenerative disorders.[16–19] For example, studies of the oxygen environment in the retinas of Royal College of Surgeons (RCS) and *P23H* rhodopsin rat models of retinal degeneration implicate oxidative stress in photoreceptor cell death,[8,20,21] and superoxide production and oxidative damage of proteins, lipids, and DNA are increased in retinas of *rd1* and *rd10* mice.[22–24] Several animal models of retinal degenerations across different mammalian species show an inverse relationship between rates of photoreceptor degeneration and the lifespan potential of the species, and lifespan is strongly correlated with mitochondrial ROS formation,[15] suggesting that mitochondrial ROS play an important and generic role in photoreceptor cell death.[17] Increased nitric oxide and superoxide anions are observed in light-induced retinal degeneration and are responsible for photoreceptor cell death.[6,25] Oxidative stress has also been implicated in pathogenesis of age-related macular degeneration (AMD).[16,18,26,27] Thus, one promising strategy for therapy development is to identify and ameliorate the sources of oxidative stress in photoreceptor degeneration.

The NADPH oxidase (NOX) family is a class of multicomponent enzymes specialized for production of superoxide radicals and other ROS.[28] Initially identified in phagocytes, ROS-

Investigative Ophthalmology & Visual Science

generating NOX has a crucial role in innate host defense against invading pathogens.[29,30] In the resting state, the NOX complex is dissociated as cytosolic subunits (p40phox, p47phox, p67phox, and small GTPase RAC1 or RAC2) and membrane central subunits (catalytic gp91phox [also termed NOX2] and its partner, p22phox).[31,32] Upon activation, the cytosolic subunits translocate to the membrane and associate with the membrane subunits for assembly of the whole complex. However, the primary function of NOX in ROS generation is not limited to phagocytes.[28,33] Several homologs of classic gp91phox (NOX2), NOX1 to 5 and dual oxidase1 and 2, have been identified in nonphagocytic cells. Nonphagocytic NOX is involved in a variety of physiologic processes and also in many pathologic conditions.[28,34–38] In nonphagocytic cells, active RAC1-GTP is thought to bind and activate p67phox, which is essential for subunit assembly and activation of NOX.[34,39] Most likely this is the case for mouse retinas, since mouse retinas express RAC1, not RAC2.[40] In addition to RAC1, other NOX components, such as the catalytic subunit (NOX1, NOX2, and NOX4) and p22phox, are also expressed in the mouse retina, including photoreceptor cells.[40–43]

Previous studies indicate that both RAC1 depletion and NOX inhibition have a similar protective effect in a light-induced photoreceptor degeneration model,[40] but the mechanisms are not clearly defined. RAC1 is a member of the Rho small GTPases and responds to extracellular stimuli by cycling between the inactive GDP-bound and active GTP-bound forms. When bound to GTP, active RAC1 binds to diverse downstream effectors to initiate a variety of biologic functions including cell polarity, migration, morphogenesis, and ROS production.[34,44–46] RAC1-induced ROS production involves the NOX family. RAC1-NOX-ROS signaling has been associated with cardiovascular and neurodegenerative diseases.[34,47–49] Given that active RAC1 is critical for assembly and activation of NOX holoenzyme, we wondered whether RAC1 activation might induce photoreceptor apoptosis by activating NOX to elevate ROS production and oxidative stress.

To investigate this hypothesis, we used our previously described transgenic mouse line, which expresses a constitutively active (CA) *Rac1* transgene specifically in rod photoreceptors under control of the *rod opsin* promoter.[50] These mice show early-age disruption of rod morphogenesis and also exhibit progressive photoreceptor degeneration with aging. Here, we have focused on the biologic role of NOX in the degeneration stages as separate from our previous description of the developmental defects observed in these transgenic (Tg)–CA-RAC1 mice. Our new findings indicate that increased NOX-mediated oxidative stress is a major factor contributing to photoreceptor degeneration in the Tg-CA-RAC1 mice. To distinguish this from degeneration due to developmental defects, we delivered the *CA Rac1* gene to the mature WT retina with a gene transfer vector. This produced photoreceptor degeneration in transduced regions, which further implicates RAC1 activity as a potential cause of some forms of rod cell death.

Methods

Transgenic Mice

We have previously generated Tg-CA-RAC1 mice by using the *rod opsin* promoter and characterized CA-RAC1 transgene expression in these mice, which occurred only in rods.[50] Transgenic-CA-RAC1 and nontransgenic WT littermates were used in the current experiments. All animal experimental protocols were approved by the National Institutes of Health Animal Care and Use Committee and adhered to the ARVO Statement for the Use of Animals in Ophthalmic and Vision Research.

Western Blot

Western blot and quantification were performed as described by Song et al.[50] Briefly, equal amounts of proteins from each sample were resolved by SDS-PAGE and analyzed by Western blot on the LI-COR Odyssey Infrared Imaging System (LI-COR Biosciences, Lincoln, NE, USA) using Odyssey software. Quantification of Tg-CA-RAC1 and endogenous (WT) RAC1 expression were performed in transgenic mice at age postnatal week (Pw) 2 ($n = 3$).

RAC1 Activity Assay

GTP-bound active RAC1 levels were determined by using G-LISA RAC1 Activation Assay Kit (Cytoskeleton, Denver, CO, USA) containing an ELISA plate coated with a RAC-GTP binding protein. GTP-bound RAC1 in cell/tissue lysates will bind to the wells, whereas inactive GDP-bound RAC1 is removed during washing steps. Briefly, freshly prepared retinal extracts containing 50 μg proteins were added to the microplate. After 30 minutes of incubation on an orbital shaker at 4°C, the plate was washed to remove inactive GDP-bound RAC1. The GTP-bound active RAC1 was detected with a RAC1-specific monoclonal antibody followed by horseradish peroxidase secondary antibody. Luminescence of each well in the plate was measured immediately on Victor 3 plate reader (Perkin-Elmer, Norwalk, CT, USA). The GTP-bound RAC1 levels in Tg-CA-RAC1 retinas were expressed as a fold change as compared to the nontransgenic WT littermate values. Each sample was analyzed in triplicate, and the data were averaged from three different animals for each genotype.

Injection With Apocynin, an Inhibitor of NOX

Groups of Tg-CA-RAC1 mice were administrated intraperitoneal (IP) injections of apocynin (10 mg/kg in PBS; Abcam, Cambridge, MA, USA)[24] daily starting at postnatal day (P) 4 for indicated periods of time (3, 7, or 13 weeks). Control groups of Tg-CA-RAC1 mice were given IP injections of PBS (vehicle).

Histology

For retinal histologic analysis with cryosections, whole eyes were fixed overnight in 4% paraformaldehyde at 4°C. Fixed eye cups were cryoprotected, embedded, snap-frozen in Tissue-Tek O.C.T. compound (Sakura Finetek USA, Inc., Torrance, CA, USA), and cryosectioned to obtain 10-μm-thick sections. Cryosections were cut through the optic nerve and were stained with hematoxylin-eosin. For retinal histologic analysis using plastic sections, eyes were fixed in 2% paraformaldehyde and 2.5% glutaraldehyde for 24 hours at 4°C. Fixed eye cups were post-fixed in 1% osmium tetraoxide for 1 hour, dehydrated in a graded ethanol series, and infiltrated overnight on a rotator in a 1:1 mixture of propylene oxide and Araldite resin (Electron Microscopy Sciences, Hatfield, PA, USA) before embedding and polymerization in freshly prepared Araldite resin for 24 hours at 60°C. Sections (0.5 μm) were cut through the optic nerve along the vertical meridian and were stained with toluidine blue. Stained sections were visualized and photographed with a Zeiss Axio Imager 2 (Carl Zeiss Microscopy, Jena, Germany). Outer nuclear layer (ONL) thickness was evaluated by counting rows of nuclei across the ONL width at 200-μm intervals in the region between 200 and 1000 μm from the optic nerve head (ONH). Counting was done in the inferior and superior halves of the retinal sections. For each genotype, three sections per animal from four animals at each age (Pw3, Pw8, and Pw13) were counted.

Investigative Ophthalmology & Visual Science

Terminal Deoxynucleotidyl Transferase–dUTP Nick-End Labeling (TUNEL) Staining

TUNEL staining was performed by using the In Situ Cell Death Detection Kit (TMR red; Roche Applied Science, Mannheim, Germany) according to the manufacturer's procedure. Briefly, fixed cryosections were incubated in permeabilization solution (0.1% Triton X-100, 0.1% sodium citrate), rinsed in PBST (0.1% Triton X-100 in PBS), and subsequently incubated with TUNEL reaction mixture. The sections were then counterstained with 4′,6′-diamidino-2-phenylindole (DAPI; Invitrogen, Eugene, OR, USA) and processed for imaging as described below in Immunohistochemistry. TUNEL-positive cells were counted in the inferior and superior halves of retinal sections from four animals at each time point (Pw3, Pw8, and Pw13).

Adeno-Associated Virus Type 8 (AAV8) Vectors and Vector Production

Myc-tagged *Rac1*^{G12V} (CA mutant, *CA Rac1*) was amplified from a cDNA clone of N-terminal *Myc*-tagged human *Rac1*^{G12V} (www.cdna.org; provided in the public domain by Missouri S&T cDNA Resource Center), which is the same cDNA clone we used to generate Tg-CA-RAC1 mice. A *Bam*HI site and a *Kozak* sequence (GCCACCATGG) were added to the 5′ end, and a *Bst*EII site was added to the 3′ end of *CA Rac1*. The following primers were used during PCR reactions: forward primer 5′-GAGAGGATCCGCCACCATGGAGCAGAAGCTGATC-3′ and reverse primer 5′-CGATTGGTCACCATCGATCGAGTTA CAACAGCAGGCATTTTC-3′. The purified PCR product was cloned into a plasmid vector (pIRES-hrGFP II; Agilent Technologies, Santa Clara, CA, USA) between a cytomegalovirus promoter and internal ribosome entry site (*IRES*) sequence. The fragment containing *CA Rac1-IRES-GFP* was removed from the plasmid with restriction endonucleases *Bam*HI and *Xho*I and was then inserted into a cis pAAV plasmid vector between a mouse *rod opsin* promoter and human *β-globin polyadenylation* (*PolyA*) sequence. The *rod opsin* promoter (*pOpsin*) was derived from upstream region between base pairs −8 to −1428 of *rod opsin* gene by using mouse tail DNA as template. The final plasmid, pAAV-*pOpsin-CA Rac1-GFP-PolyA*, was used to make the recombinant AAV8 virus vector. The plasmid pAAV-*pOpsin-GFP* vector was used to make the control virus vector.

Recombinant adeno-associated viruses were produced by the triple transfection method and purified by polyethylene glycol precipitation followed by cesium chloride density gradient fractionation. The method has been previously described.[51] The purified virus vectors were formulated in 10 mM Tris-HCl, 180 mM NaCl (pH 7.4) and 0.001% Pluronic F-68 (pH 7.4; Life Technologies, Carlsbad, CA, USA) and stored at −80°C. Quantification of vectors was done by real-time PCR by using linearized plasmid standards.

Subretinal Injection of AAV8 Vectors

Mice at Pw6 were anesthetized with IP injection of ketamine (80 mg/kg) and xylazine (10 mg/kg), and 0.5% tetracaine was applied topically to the eye. Animals were placed under a dissecting microscope with the injected eye facing up. The conjunctiva membrane at the injection area was opened. A small incision was made by a sterile 33-gauge sharp needle (TSK Laboratory, Tochigi, Japan) passing through the sclera, choroid, and retinal pigment epithelium (RPE) to reach the subretinal space. Approximately 1 μL AAV8 virus vectors (2.9×10^{12} vg/mL) was introduced into the subretinal space with a blunt 35-gauge needle attached to a 10-μL Nanofil syringe (World Precision Instruments, Inc., Sarasota, FL, USA). After injections, the needle was carefully withdrawn from the eye, and triple antibiotic ophthalmic ointment (neomycin, polymixin B, and bacitracin) was applied. Retinal morphology was analyzed 10 weeks after injection.

Immunohistochemistry

Eyes were fixed in 4% paraformaldehyde for 2 hours at 4°C. Fixed eye tissues were cryoprotected, embedded, snap-frozen in Tissue-Tek O.C.T. compound, and cryosectioned at 10-μm thickness. Cryosections were washed in PBST and blocked in blocking buffer (20% goat serum and 0.5% Triton X-100 in PBS). Then, the slides were incubated with anti-MYC-tag (Cell Signaling Technology, Danvers, MA, USA) primary antibody overnight at 4°C, washed in PBST, and incubated with anti-rabbit Alexa Fluor 568 secondary antibody (1:1000; Invitrogen). Retinal nuclei were counterstained with DAPI and sections were mounted in Fluoro-Gel buffer (Electron Microscopy Sciences, Hatfield, PA, USA) for imaging. The images were generated and analyzed by the Nikon C2 Confocal Microscope (Nikon, Tokyo, Japan) with NIS-elements AR software, and further edited with Adobe Photoshop CS4, version 11.0 (Adobe Systems, Inc., San Jose, CA, USA). The ONL thickness was evaluated by counting rows of nuclei across the ONL width in photomicrographs of retinal sections. In AAV8-*pOpsin-CA Rac1-GFP*–injected retinas, nuclei were counted at 400-μm intervals in the regions with CA RAC1-GFP–stained cells and regions with no CA RAC1-GFP–stained cells. In AAV8-*pOpsin-GFP*–injected retinas, nuclei were counted at 400-μm intervals in the regions with GFP-stained cells. In a single retinal section, the nuclei counts at each point in the defined regions were averaged to give an overall estimate of the ONL thickness for that retinal region. Quantification was done on two or three sections per animal from four animals for each group.

Evaluation of Superoxide Production

Production of *in situ* superoxide in the retina was assessed by using a superoxide-sensitive fluorescent dye (dihydroethidium [DHE])–based procedure described previously.[24,52] Briefly, mice were administered IP injections of freshly prepared DHE (20 mg/kg; Life Technologies, Eugene, OR, USA) and euthanized after 18 hours. Eyes were rapidly enucleated, embedded, and snap-frozen in Tissue-Tek O.C.T. compound and cryosectioned to obtain 10-μm-thick sections. Cryosections were fixed in 4% paraformaldehyde for 20 minutes at room temperature and washed in PBS. Retinal nuclei were counterstained with DAPI and sections were mounted in Fluoro-Gel buffer for imaging. The images were generated and analyzed with a Nikon C2 Confocal Microscope with NIS-elements AR software, and further edited by using Adobe Photoshop CS4, version 11.0. All sections were imaged with the same settings. Fluorescence intensity was used to indicate superoxide levels. Pixel intensity was measured along the entire length of the ONL in photomicrographs of retinal sections by using ImageJ software (http://imagej.nih.gov/ij/; provided in the public domain by the National Institutes of Health, Bethesda, MD, USA), as previously described.[53] Pixel intensity measurement was done on three animals for each group at Pw3, and at least two sections per animal were measured.

Measurement of Protein Carbonyls

Protein carbonyl content was measured immunochemically by derivatizing proteins with the carbonyl reagent 2,4 dinitrophenylhydrazine (DNPH) according to the method described by Wehr and Levine.[54] Total retinal proteins were extracted in 20

mM Tris-HCl, 150 mM NaCl (pH 7.4) buffer, and protein concentrations were determined by using the BCA Protein Assay Kit (Thermo Fisher Scientific, Waltham, MA, USA). Retinal extracts (equal amounts of proteins) were mixed with 1 volume of 12% SDS followed by 2 volumes of 20 mM DNPH (Spectrum Chemical, New Brunswick, NJ, USA) in 10% trifluoroacetic acid (TFA; Thermo Fisher Scientific). For blanks, samples were mixed with 2 volumes of 10% TFA alone. After 10 minutes of incubation at room temperature, the samples were neutralized by adding 1.7 volumes of 2 M Tris–30% glycerol. On SDS-PAGE, equal amounts of total proteins were loaded in each lane of the individual gels and the samples were promptly subjected to electrophoresis and blotting. The blots were probed by using goat anti-DNP affinity-purified antibody (Bethyl Laboratories, Inc., Montgomery, TX, USA) followed by donkey anti-goat IR Dye 800CW (LI-COR Biosciences) secondary antibody. Blots were scanned on the LI-COR Odyssey Infrared Imaging System and analyzed by using Odyssey software. Quantification was made in three mice for each of apocynin- and vehicle-injected groups at Pw7. For each lane, band intensity of each protein corresponding to the bands around 180, 150, 100, 75, 60, 50, 37, and 25 kDa was quantified and normalized to actin. All values were totaled to provide an overall estimate. The data are expressed in relative terms.

Thiobarbituric Acid Reactive Substances (TBARS) Assay

Malondialdehyde (MDA) concentrations were determined colorimetrically following its controlled reaction with thiobarbituric acid by using a TBARS (TCA Method) Assay Kit (Cayman Chemical Company, Ann Arbor, MI, USA).[55,56] Two retinas were pooled for each group for each assay, and the assay was repeated three times. Retinas were sonicated in RIPA buffer (Cayman) containing a protease inhibitor cocktail. The lysates were centrifuged and the supernatant was used for the TBARS assay. The assay was performed in duplicate according to the manufacturer's protocol. A standard curve was prepared by using MDA samples of known concentration. Malondialdehyde concentrations in test samples were extrapolated from the standard curve and expressed in μM MDA/mg retinal extract.

Electroretinography (ERG)

Full-field (Ganzfeld) scotopic ERGs were recorded from apocynin- and vehicle-injected Tg-CA-RAC1 mice at Pw13 by using an Espion E2 Electrophysiology System with a Color-Dome Ganzfeld stimulus (Diagnosys LLC, Lowell, MA, USA). All animals were dark adapted for at least 12 hours before ERG recording. Mice were anesthetized with IP injection of ketamine (80 mg/kg) and xylazine (10 mg/kg) under dim red light. Pupils were dilated with topical 0.5% tropicamide and 0.5% phenylephrine HCl. The cornea was kept moist with methylcellulose solution. A gold wire was placed on the moistened cornea as a recording electrode, and a gold reference electrode was placed in the mouth. A needle electrode inserted subcutaneously close to the tail served as ground. Electroretinograms were recorded simultaneously from both eyes at bandwidths of 0.1 to 500 Hz. Dark-adapted ERGs were elicited by a series of white single flashes from −4.8 to +2.25 log cd-s/m^2. A-wave amplitude was measured from the prestimulus baseline to the initial negative trough at intensities from −1.8 to +2.25 log cd-s/m^2 flash. B-wave amplitude was measured from the baseline, or from the a-wave trough when present, to the peak at intensities from −4.8 to −0.3 log cd-s/m^2 flash. A- and b-wave amplitudes at every intensity were averaged from both eyes and compared between apocynin- and vehicle-injected Tg-CA-RAC1 mice. Measurements were made on four animals for each treatment group.

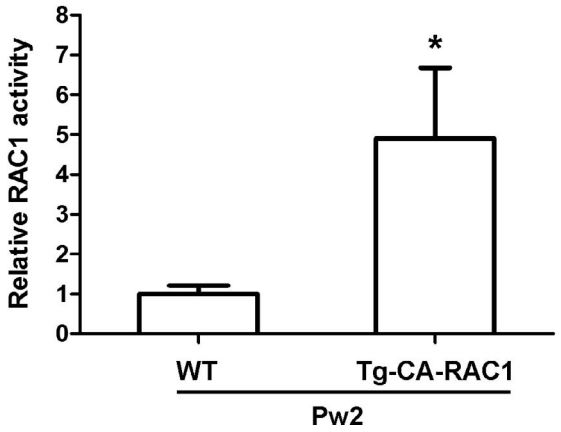

FIGURE 1. RAC1 activity is increased in Tg-CA-RAC1 mice. RAC1 activity (GTP-bound active RAC1) was assessed in retinas by using a RAC1 activation assay (see Methods). Luminescence values of the RAC1-GTP in each sample at Pw2 were normalized to luminescence values of the RAC1-GTP in WT controls. Relative RAC1 activity in Tg-CA-RAC1 retinas is represented as a fold change compared to WT controls as shown in the *bar graph* (4.9 ± 1.8, $^*P < 0.05$, $n = 3$).

Statistical Analysis

Quantitative data are presented as mean ± SEM. The average number of nuclei across the ONL width in WT and Tg-CA-RAC1 mice at different ages was compared by using 1-way ANOVA in GraphPad Prism 6.01 for Windows (GraphPad Software, La Jolla, CA, USA). Statistical comparison of a- and b-wave amplitudes across a range of stimulus intensities was done by using the *t*-test and correcting for multiple comparisons with the Holm-Sidak method in GraphPad Prism 6.01 for Windows. All other statistical analyses between two groups were carried out by using Student's *t*-test.

RESULTS

Constitutively Active RAC1 Expression in Rods Induces Photoreceptor Degeneration in Tg-CA-RAC1 Mice

We have previously characterized CA-RAC1 transgene expression in transgenic mice at very early age.[50] Here we further examined Tg-CA-RAC1 protein expression at Pw2 with Western blot. By Pw2, CA-RAC1 expression reached 126.5% ± 6.1% of endogenous RAC1 level in Tg-CA-RAC1 mice. We also evaluated RAC1 activity in the transgenic retina by using RAC1 activation assay and found that the level of active RAC1-GTP was increased 5-fold (4.9 ± 1.8, $P < 0.05$, $n = 3$) in Tg-CA-RAC1 mice at Pw2, compared to WT littermates (Fig. 1).

Histology of retinal sections showed that Tg-CA-RAC1 retinas had progressively fewer photoreceptor cells from Pw3 (ONL rows/retina: 7.85 ± 0.18, $n = 4$) to week 13 (4.5 ± 0.15 at Pw8, $n = 3$; 1.8 ± 0.04 at Pw13, $n = 4$; $P < 0.0001$) as compared with WT controls at Pw3 (10.83 ± 0.03, $n = 3$) (Figs. 2A, 2B). Retinal sections were also examined by TUNEL assay at three different ages (Pw3, Pw8, and Pw13), and Tg-CA-RAC1 retinas had a greater number of apoptotic cells in the ONL at all three ages than did WT control retinas, which showed nearly no TUNEL-positive cells in any layers (Figs. 2C,

Investigative Ophthalmology & Visual Science

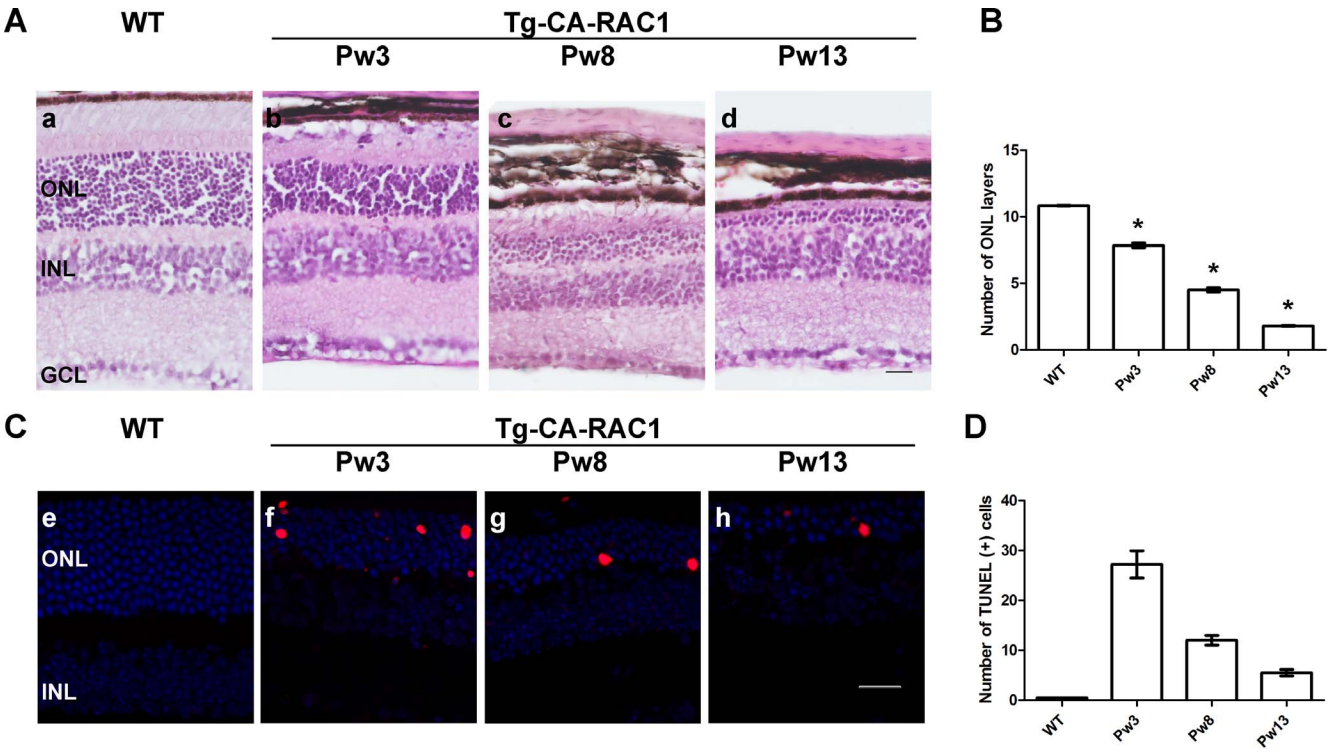

FIGURE 2. Transgenic-CA-RAC1 mice develop progressive photoreceptor degeneration from Pw3 to Pw13. (**A**) Retinal sections stained by hematoxylin-eosin and (**B**) row counts of nuclei across the ONL width in WT (**a**) and Tg-CA-RAC1 mice at several postnatal times (Pw3 [**b**], Pw8 [**c**], and Pw13 [**d**]) showed progressive photoreceptor cell loss with aging ($^*P < 0.01$, $n = 4$). *Scale bar*: 20 μm. (**C**) Retinal sections of WT (**e**) and Tg-CA-RAC1 mice at Pw3 (**f**), Pw8 (**g**), and Pw13 (**h**) by TUNEL assay. (**D**) TUNEL-positive (*red*) cell counts indicated increased apoptosis signals in the ONL at all three ages as compared with WT controls, which showed nearly no TUNEL-positive cells in any layers. *Scale bar*: 20 μm. ONL, outer nuclear layer; INL, inner nuclear layer; GCL, ganglion cell layer.

2D). These results indicate that extensive photoreceptor degeneration by apoptosis occurs in Tg-CA-RAC1 retina between Pw3 and Pw13.

Inhibiting NOX Reduces Superoxide Accumulation and Oxidative Stress in Tg-CA-RAC1 Retinas

Active RAC1 is critical for activation of NOX in nonphagocytic cells including neurons,[34,48,57] which leads to production of ROS, primarily of superoxide radicals. We examined superoxide production in the retina by using DHE. Dihydroethidium is a fluorescent indicator of superoxide radicals and is a standard fluorescent probe for determining nonphagocytic NOX activity.[24,52,58] At Pw3, the ONL of Tg-CA-RAC1 retinas still had a large number of photoreceptors and showed stronger oxidized DHE fluorescence (red) than WT retinas (Figs. 3A, 3B). To determine whether NOX activation contributes to superoxide accumulation in Tg-CA-RAC1 retinas, Tg-CA-RAC1 mice were treated with daily IP injections of apocynin, a NOX inhibitor, for ~3 weeks. The ONL of apocynin-treated Tg-CA-RAC1 retinas showed significantly less fluorescence than vehicle-injected Tg-CA-RAC1 mice, which gave a pattern similar to uninjected Tg-CA-RAC1 retinas (Figs. 3A, 3B). These results implicate NOX activation as contributing to increased superoxide production in Tg-CA-RAC1 retinas.

Protein carbonylation is a general indicator of protein oxidation and is a marker for oxidative stress.[54,59] To learn whether increased NOX-mediated ROS production results in oxidative damage, we treated the Tg-CA-RAC1 mice with IP injections of apocynin or vehicle control daily for 7 weeks and assessed retinal protein carbonyl content by Western blot (Fig. 4A). Apocynin-treated Tg-CA-RAC1 retinas had significantly lower levels of protein carbonyls than vehicle treatment (Fig. 4B). We also measured MDA levels in the retinas to evaluate lipid peroxidation during oxidative stress. Malondialdehyde has been used as a biomarker for oxidative stress.[56,60,61] Malondialdehyde was decreased by 61% ± 4% ($P < 0.01$) in apocynin-treated Tg-CA-RAC1 retinas compared with vehicle treatment (Fig. 4C). Both results indicate that increased NOX activity contributes to oxidative damage in Tg-CA-RAC1 retinas.

Delivering CA-RAC1 to the Mature WT Retina Produces Photoreceptor Degeneration

We have previously shown that rod morphogenesis is disrupted in transgenic CA-RAC1 mice,[50] and it is possible that these developmental defects could be the cause of photoreceptor degeneration in Tg-CA-RAC1 retinas. Thus, we explored whether CA-RAC1 expression in rods of WT mice could induce photoreceptor degeneration in the retina independent of any developmental defects. To study this, we administered AAV8-*pOpsin-CA Rac1-GFP* by subretinal injection in adult WT mice to target CA-RAC1 expression to normal rods at 6 weeks of age. This approach gave ONL regions with AAV8-*pOpsin-CA Rac1-GFP*–transduced photoreceptors while other regions were not transduced, all within a single retina. Hence we could compare CA-RAC1–expressing ONL regions with non–CA RAC1-expressing ONL regions side by side in the same retina (Figs. 5B, 5C). The ONL regions containing rod photoreceptors that were not transduced with *CA Rac1* were used as internal controls. Significantly fewer ONL cells were seen in areas with *CA Rac1-GFP*–transduced photoreceptors than in regions not transduced (Fig. 5D). As an additional control, AAV8-*pOpsin-GFP* vector was injected

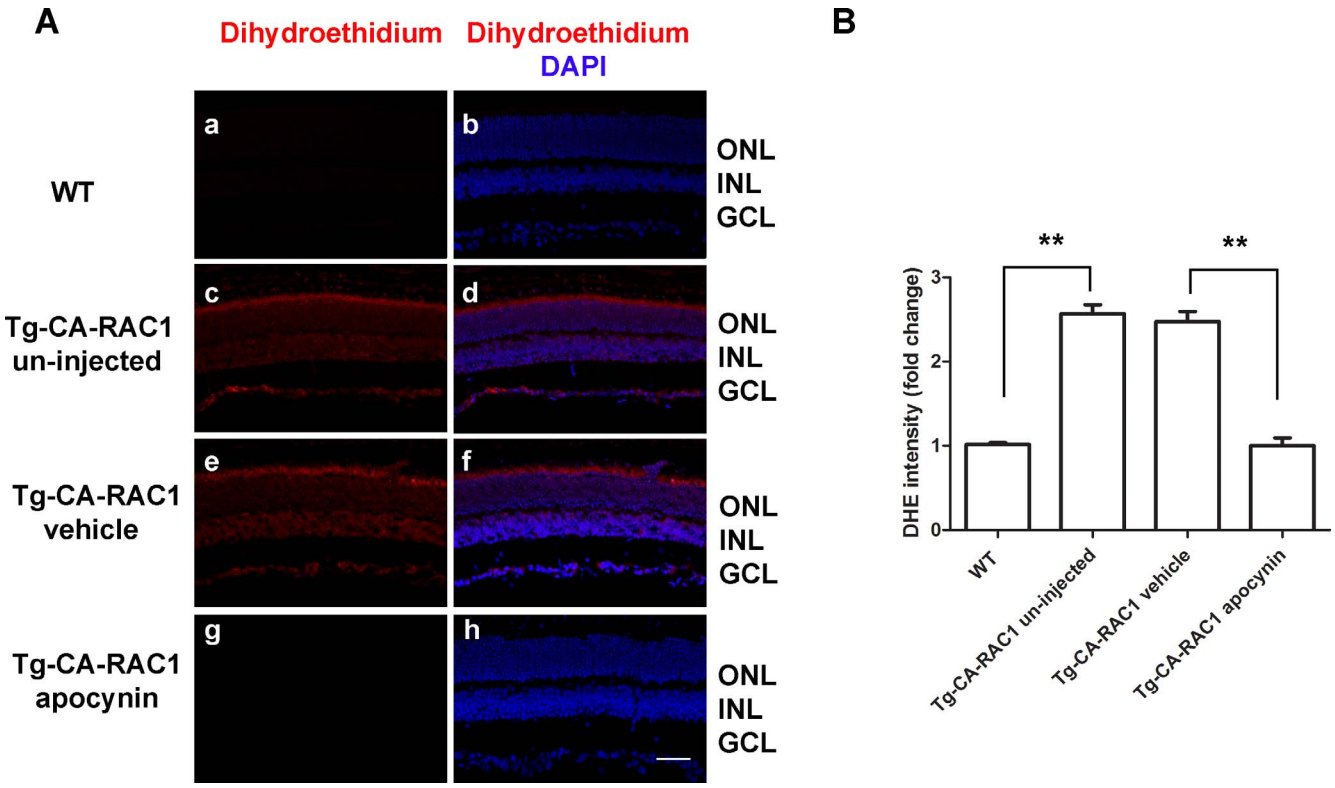

FIGURE 3. Apocynin, a NOX inhibitor, reduces superoxide accumulation in Tg-CA-RAC1 retinas. Transgenic-CA-RAC1 mice were given daily IP injections of apocynin or vehicle control for ~3 weeks starting at P4. At the end of Pw3, mice were injected intraperitoneally with DHE (20 mg/kg) and euthanized after 18 hours. Retinal sections were examined by confocal microscopy. (**A**) Representative images of the retinal sections are shown. Compared to the WT control (**a**, **b**), uninjected Tg-CA-RAC1 retina (**c**, **d**) had stronger oxidized DHE staining (*red*) in the ONL layer. Apocynin-injected Tg-CA-RAC1 retina (**g**, **h**) showed much less *red staining* than vehicle-injected Tg-CA-RAC1 retina (**e**, **f**), which had similar *red staining* to that shown in uninjected Tg-CA-RAC1 retina (**c**, **d**). *Scale bar*: 50 μm. (**B**) Dihydroethidium fluorescence intensity of the ONL region was measured in the WT, uninjected Tg-CA-RAC1, vehicle-injected Tg-CA-RAC1, and apocynin-injected Tg-CA-RAC1 retinas. Dihydroethidium intensity values of each sample were normalized to DHE values of WT samples. Quantification of DHE intensity is represented as a fold change compared to WT retinas in the *bar graph* (**$P < 0.001$, $n = 3$). The data indicate that NOX contributes to superoxide production in Tg-CA-RAC1 retinas.

into retinas of another group of mice, and no significant cell loss was observed in these *GFP*-transduced retinas (Figs. 5A, 5C, 5D). Together with results in the transgenic retina, these data implicate CA-RAC1 expression in photoreceptor degeneration.

Inhibiting NOX Protects Photoreceptors and Rescues Rod Function

At this point we could conclude that NOX contributed to ROS generation and oxidative stress in Tg-CA-RAC1 retinas. Thus, we explored whether inhibiting NOX would be protective. Transgenic-CA-RAC1 mice were administered apocynin IP daily for 13 weeks. Retinal morphology by plastic sections demonstrated that apocynin-treated Tg-CA-RAC1 mice retained significantly more ONL nuclei at 13 weeks of age (ONL rows/retina: 3.65 ± 0.43, $n = 4$) than vehicle controls (1.87 ± 0.33, $n = 4$; $P < 0.01$) (Figs. 6A, 6B). Vehicle injection did not rescue ONL cell number, as the number of photoreceptor cells in vehicle-injected Tg-CA-RAC1 retinas was similar to uninjected Tg-CA-RAC1 retinas (1.80 ± 0.04 at Pw13, $n = 4$, $P = 0.7$; Figs. 2A, 2B). The a- and b-wave amplitudes of the dark-adapted ERG in apocynin-injected Tg-CA-RAC1 mice ($n = 4$) were significantly larger by 3- and 2.6-fold ($P < 0.01$ and $P < 0.01$), respectively, than those of vehicle-injected Tg-CA-RAC1 controls ($n = 4$) (Fig. 6C). Thus, NOX inhibition increased the survival of photoreceptor cells and partially rescued rod function.

DISCUSSION

Active RAC1 is known to be an important regulator of NOX activity in nonphagocytic cells including neurons.[34,48,49,57,62] We investigated whether activated RAC1 induces oxidative stress in mouse rod photoreceptors, by increasing NOX-mediated ROS generation, and contributes to rod degeneration. We found that expression of CA-RAC1 under control of a *rod opsin* promoter in transgenic mice enhanced retinal superoxide production and rod degeneration. We have previously shown that the development of some rods is disrupted in Tg-CA-RAC1 mice and that progressive photoreceptor degeneration is observed with aging in these mice.[50] However, based on that study and the current study, it is unlikely that these degenerative defects reflect only developmental issues. First, only a portion of the rods expressing CA-RAC1 exhibited morphologic defects, while extensive photoreceptor cell loss occurred progressively throughout the ONL in adult Tg-CA-RAC1 retinas. Second, we found that CA-RAC1 expression can induce photoreceptor degeneration in ONL regions of mature WT retinas transduced with AAV8-*pOpsin-CA Rac1-GFP* (Fig. 5). Additionally, inhibiting NOX significantly reduced the level of superoxide radicals and protein and lipid oxidation in Tg-CA-RAC1 retinas, and partially rescued retinal morphology and rod function. Collectively, our data indicate that NOX-mediated oxidative stress contributes to rod photoreceptor degeneration in Tg-CA-RAC1 mice.

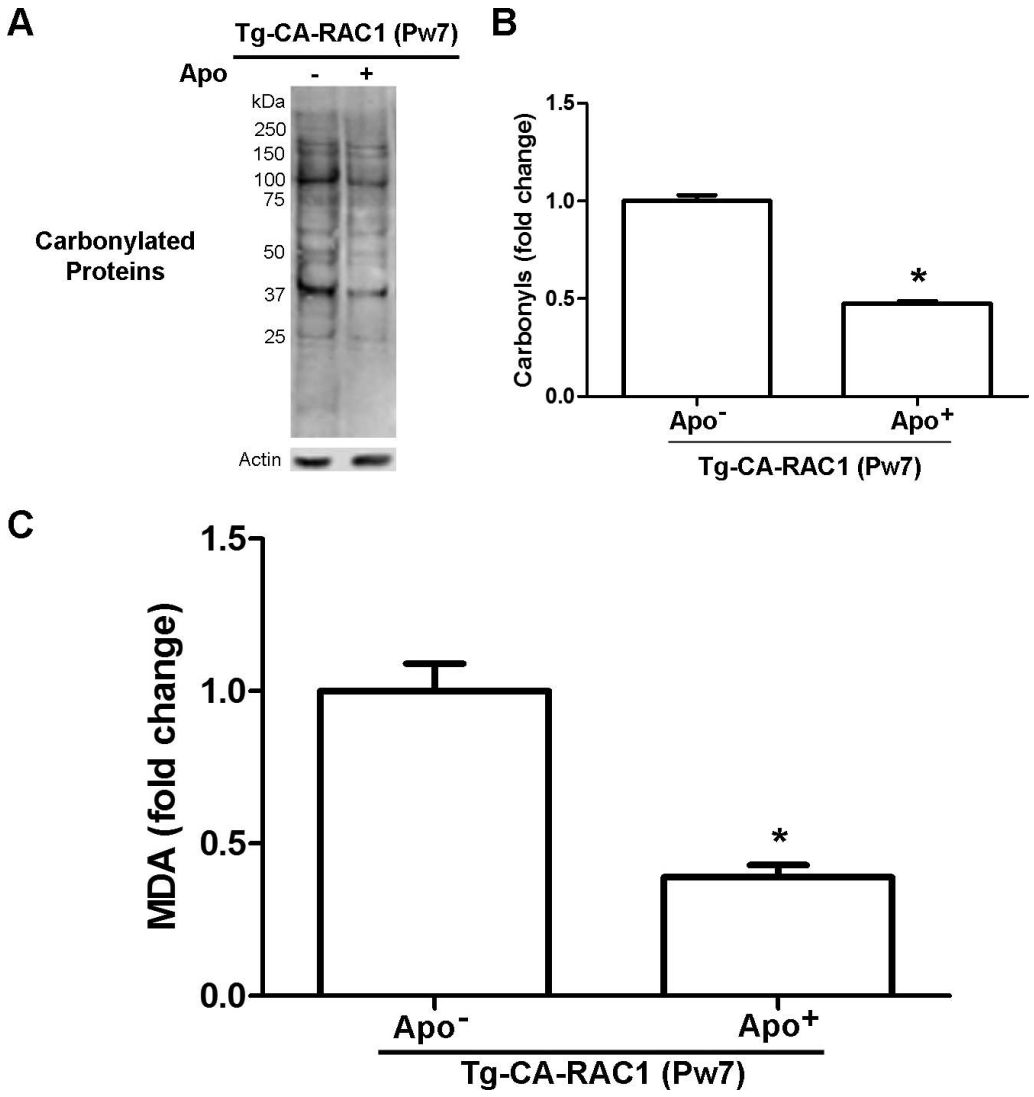

Figure 4. Apocynin attenuates oxidative damage in Tg-CA-RAC1 retinas. Transgenic-CA-RAC1 mice were given daily IP injections of apocynin or vehicle control for ~7 weeks starting at P4. Mice were euthanized at Pw7. (**A**) Equal amounts of proteins from retinal extracts of vehicle-injected (Apo^-) and apocynin-injected (Apo^+) Tg-CA-RAC1 mice were analyzed by Western blot for protein carbonylation, a marker for oxidative stress. Western blots with anti-DNP antibody show carbonylated proteins in retinal extracts of Tg-CA-RAC1 (Apo^- and Apo^+) mice. Actin is used as an additional control for Western blot. (**B**) Fluorescence values of each carbonylated protein band (180, 150, 100, 75, 60, 50, 37, 25 kDa in [**A**]) were normalized to fluorescence values of corresponding actin band and then totaled to provide an overall estimate. Total protein carbonyl content of apocynin-injected Tg-CA-RAC1 (Apo^+) retinas is represented as a fold change compared to that in vehicle-injected Tg-CA-RAC1 (Apo^-) retinas (0.5 ± 0.08, $^*P < 0.01$, $n = 3$). (**C**) A TBARS assay was performed to measure the levels of MDA, a marker of oxidative stress and lipid peroxidation, in vehicle-injected (Apo^-) and apocynin-injected (Apo^+) Tg-CA-RAC1 retinas. Data are represented as a fold change in MDA concentrations compared to those in vehicle-injected Tg-CA-RAC1 (Apo^-) retinas (0.39 ± 0.04, $^*P < 0.01$, $n = 3$). Both results indicate that NOX activation contributes to oxidative damage in Tg-CA-RAC1 retinas.

The ability of transgenic CA-RAC1 in photoreceptors to increase superoxide radicals and induce oxidative damage, leading to their degeneration, indicates that endogenous RAC1 activation may play an important role in environmentally induced and in inherited photoreceptor degenerations. In the light-induced model of photoreceptor degeneration in mouse, superoxide radicals and other ROS contribute to photoreceptor apoptosis[25] and RAC1 has been linked to photoreceptor cell loss.[40,63] A recent study[64] has found that NOX mediates ROS generation and oxidative damage in mouse photoreceptors after blue light damage. In addition, RAC1-NOX–dependent superoxide generation is responsible for light-induced degeneration of Crumbs-deficient photoreceptor cells in *Drosophila*.[65] In the present study, we demonstrated that NOX contributes to increased superoxide accumulation, oxidative damage, and photoreceptor cell death in Tg-CA-RAC1 retinas. All these studies support the idea that RAC1 activation contributes to light-induced photoreceptor degeneration by triggering ROS generation through its regulation of NOX activity in rods. As a result, both RAC1 depletion and NOX inhibition have a similar protective effect on rods against light damage.[40]

Recent findings demonstrate that NOX-derived ROS and oxidative damage are implicated in photoreceptor cell death in *rd1* and *Q344ter* rhodopsin mouse genetic models of retinal degeneration.[24] Other cell types in the retina with NOX activity include RPE and ganglion cells.[41,42] Reduced p22phox level in RPE cells, a membrane subunit of the NOX complex, inhibits choroidal neovascularization and suggests a role for NOX in neovascularization in AMD.[41] In mouse retina, NOX expression

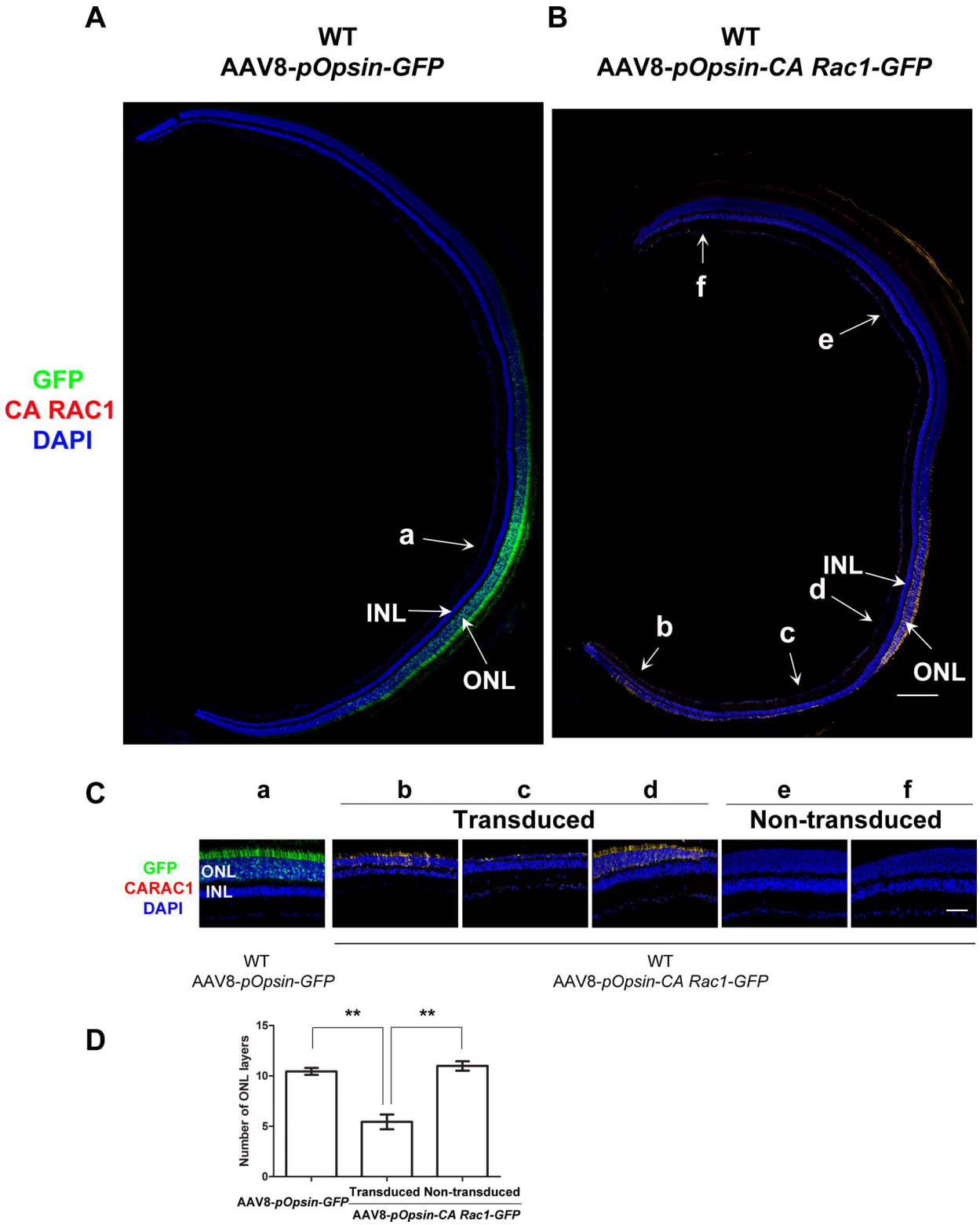

Figure 5. Expression of CA-RAC1 in adult WT photoreceptors induces photoreceptor degeneration. AAV8-*pOpsin-CA Rac1-GFP* or control AAV8-*pOpsin-GFP* vectors were delivered subretinally to Pw6 WT eyes. Retinal morphology was evaluated 10 weeks after injections. Retinal sections were immunostained with antibody against MYC-tag (*red*, CA RAC1). Retinal nuclei were labeled with DAPI (*blue*). In total, four animals for each vector were examined. As shown in representative cross-sections of AAV8-*pOpsin-GFP*–injected (**A**) and AAV8-*pOpsin-CA Rac1-GFP*–injected (**B**) retinas, at least one-third of the entire length of the ONL regions was transduced by AAV8 vectors. In AAV8-*pOpsin-CA Rac1-GFP*–injected animals (**B**), both *CA RAC1-GFP*–transduced (**b**, **c**, **d**; *yellow*) and non–*CA RAC1-GFP*-transduced (**e**, **f**) ONL regions were observed in a single retina. Thus, the ONL regions with no *CA Rac1-GFP*–transduced photoreceptors serve as internal controls. *Scale bar*: 200 μm. (**C**) High magnification images of regions ([**a** in **A**] and [**b**, **c**, **d**, **e**, **f** in **B**]) are shown. *Scale bar*: 50 μm. In AAV8-*pOpsin-CA Rac1-GFP*–injected retinas (**B**), *CA Rac1-GFP*–transduced regions (**b**, **c**, **d**; *yellow*) show significant ONL cell loss (compare [**b**, **c**, **d** in **B**] with [**a** in **A**]). In contrast, no cell loss was observed in non–*CA Rac1-GFP*-

transduced regions (**e**, **f**), which had similar ONL thickness to those in control *GFP*-transduced regions (**a**). (**D**) The ONL thickness was evaluated as described in Methods. Average row counts of nuclei across the ONL width are shown in control *GFP*-transduced (AAV8-*pOpsin-GFP*), *CA Rac1-GFP*–transduced, and non–*CA Rac1-GFP*-transduced regions (**$P < 0.001$, $n = 4$). There are significantly fewer ONL nuclei in *CA Rac1*–transduced regions than in control *GFP*-transduced regions. In AAV8-*pOpsin-CA Rac1-GFP*–injected retinas, *CA Rac1*–transduced regions show significantly fewer ONL nuclei than non–*CA Rac1*-transduced regions.

and function have been reported in microglia and in vascular endothelial cells where it may contribute to neovascularization and retinopathy of prematurity.[66–69] Microglial NOX activation also has been reported to promote photoreceptor degeneration in *rd1* mice, a model of retinitis pigmentosa (RP).[70] As visual cell apoptosis induced by oxidative stress is a shared feature of genetic and light-induced retinal degeneration and AMD,[6,71] it is warranted to evaluate whether the protective effect of RAC1 inhibition in light damage model can be extended to RP and to AMD models.

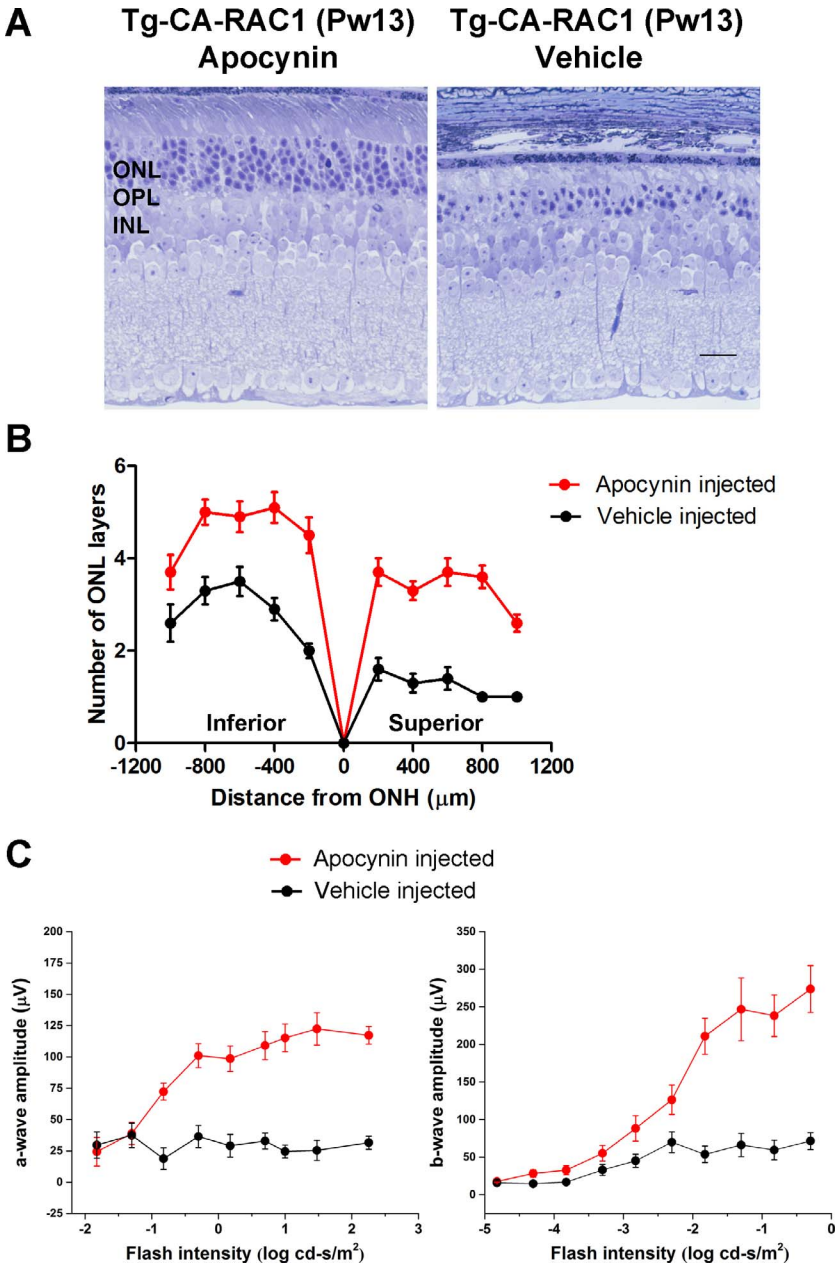

Figure 6. Apocynin rescues photoreceptor cells and rod function. Transgenic-CA-RAC1 mice were intraperitoneally injected daily with apocynin or vehicle control starting at P4 and euthanized at Pw13. (**A**) Retinal morphology is shown by toluidine blue–stained plastic sections cut through the ONH along the vertical meridian. *Scale bar*: 20 μm. (**B**) The ONL thickness is evaluated by counting rows of nuclei across the ONL width at 10 points along the retinal length of plastic sections containing ONH. Apocynin-injected Tg-CA-RAC1 mice had significantly more photoreceptor cells than vehicle-injected Tg-CA-RAC1 mice ($P < 0.01$, $n = 4$). (**C**) Retinal responses were measured by dark-adapted ERG before the mice were euthanized. Amplitude versus log intensity (V-log I) curve of dark-adapted ERG recordings shows that apocynin-injected Tg-CA-RAC1 mice had significantly larger a- and b-wave amplitudes than vehicle-injected mice ($P < 0.01$ and $P < 0.01$, respectively; $n = 4$).

RAC1-NOX signaling-mediated rod cell death in light-induced retinal degeneration is consistent with its role in other neurodegenerative diseases. RAC1 activation and NOX2 activity are elevated in primary HD140Q/140Q neurons (HD – Huntington's disease).[49] This study suggests that increased RAC1 activity accounts for increased NOX2 activity and ROS levels in human and mouse HD140Q/140Q brain and that these contribute to oxidative stress and neuronal cell death in Huntington's disease. In addition, diabetes-induced RAC1-NOX2 activation plays an important role in the development of diabetic retinopathy.[72] Intriguingly, these studies point out the possibility that RAC1-mediated NOX2 activation is an early signaling event for increasing ROS before the onset of mitochondrial dysfunction and cell apoptosis, and thus, they provide useful information for developing therapeutic approaches to reduce oxidative damage in such disorders.

Apocynin is a well-known inhibitor of NOX[73] and is often used to demonstrate NOX involvement in ROS formation in the retina.[24,70,74,75] However, Heumuller et al.[76] report that it fails to inhibit superoxide generation by NOX that is overexpressed in endothelial cells in vitro. These cells lack myeloperoxidase (MPO), which is normally required for apocynin activation,[77] and apocynin activation is not observed in MPO-free vascular endothelial cells and smooth muscle cells.[76] But, redox-sensitive processes are inhibited by apocynin, and the authors indicate that apocynin does not block NOX but predominantly acts as an antioxidant (a scavenger of peroxide-dependent ROS) in these MPO-free vascular cells. However, this is unlikely to be the mechanism in our study. First, we found that apocynin did reduce superoxide production in Tg-CA-RAC1 retinas (Figs. 3A, 3B). Second, MPO is expressed in the mouse retina, including photoreceptor cells, under inflammatory stress.[78] Third, using methods other than apocynin, it has been shown that NOX contributes to RAC1-induced ROS overproduction in nonphagocytic cells such as neurons and retinal cells.[48,72] Taken together, these facts support the idea that the inhibitory action of apocynin that we observed in Tg-CA-RAC1 retinas is predominately through NOX.

In conclusion, our data implicate activated RAC1-NOX–mediated ROS and oxidative stress in photoreceptor cell death and illuminate the potential molecular mechanism underlying neuroprotection by RAC1 inhibition and rod-specific depletion in retinal light damage. Light can activate RAC1 in the retina,[63,79] and light has been shown to enhance degeneration in several mouse genetic models of photoreceptor degeneration, for example, *P23H* and *S334ter* rhodopsin models,[80] suggesting it may be a cofactor in many retinal diseases.[6] In addition, photo-oxidative damage is thought to serve as a contributory factor to AMD.[6,71] As ROS and oxidative stress are likely involved in multiple forms of retinal degenerations, we propose that investigating RAC1 inhibition is particularly relevant as a therapeutic approach that targets this pathway in retinal diseases.

Acknowledgments

The authors thank Maria Santos and Jinbo Li for technical assistance; Rong Wen (Bascom Palmer Eye Institute, University of Miami) and Brian Brooks (National Eye Institute [NEI], National Institutes of Health [NIH]) for giving critical comments on the manuscript.

Supported by the NIH Intramural Research Programs of the National Institute on Deafness and Other Communication Disorders and the NEI, Bethesda, Maryland, United States.

Disclosure: **H. Song**, None; **C. Vijayasarathy**, None; **Y. Zeng**, None; **D. Marangoni**, None; **R.A. Bush**, None; **Z. Wu**, None; **P.A. Sieving**, None

References

1. Chang GQ, Hao Y, Wong F. Apoptosis: final common pathway of photoreceptor death in rd, rds, and rhodopsin mutant mice. *Neuron*. 1993;11:595–605.
2. Portera-Cailliau C, Sung CH, Nathans J, Adler R. Apoptotic photoreceptor cell death in mouse models of retinitis pigmentosa. *Proc Natl Acad Sci U S A*. 1994;91:974–978.
3. Reme CE, Grimm C, Hafezi F, Marti A, Wenzel A. Apoptotic cell death in retinal degenerations. *Prog Retin Eye Res*. 1998;17:443–464.
4. Travis GH. Mechanisms of cell death in the inherited retinal degenerations. *Am J Hum Genet*. 1998;62:503–508.
5. Hao W, Wenzel A, Obin MS, et al. Evidence for two apoptotic pathways in light-induced retinal degeneration. *Nat Genet*. 2002;32:254–260.
6. Wenzel A, Grimm C, Samardzija M, Reme CE. Molecular mechanisms of light-induced photoreceptor apoptosis and neuroprotection for retinal degeneration. *Prog Retin Eye Res*. 2005;24:275–306.
7. Yu DY, Cringle SJ, Alder VA, Su EN. Intraretinal oxygen distribution in rats as a function of systemic blood pressure. *Am J Physiol*. 1994;267:H2498–H2507.
8. Yu DY, Cringle SJ. Retinal degeneration and local oxygen metabolism. *Exp Eye Res*. 2005;80:745–751.
9. Stone WL, Farnsworth CC, Dratz EA. A reinvestigation of the fatty acid content of bovine, rat and frog retinal rod outer segments. *Exp Eye Res*. 1979;28:387–397.
10. Bazan NG. The metabolism of omega-3 polyunsaturated fatty acids in the eye: the possible role of docosahexaenoic acid and docosanoids in retinal physiology and ocular pathology. *Prog Clin Biol Res*. 1989;312:95–112.
11. Bush RA, Reme CE, Malnoe A. Light damage in the rat retina: the effect of dietary deprivation of N-3 fatty acids on acute structural alterations. *Exp Eye Res*. 1991;53:741–752.
12. Winkler BS. An hypothesis to account for the renewal of outer segments in rod and cone photoreceptor cells: renewal as a surrogate antioxidant. *Invest Ophthalmol Vis Sci*. 2008;49:3259–3261.
13. Finkel T, Holbrook NJ. Oxidants, oxidative stress and the biology of ageing. *Nature*. 2000;408:239–247.
14. Pettmann B, Henderson CE. Neuronal cell death. *Neuron*. 1998;20:633–647.
15. Wright AF, Jacobson SG, Cideciyan AV, et al. Lifespan and mitochondrial control of neurodegeneration. *Nat Genet*. 2004;36:1153–1158.
16. Beatty S, Koh H, Phil M, Henson D, Boulton M. The role of oxidative stress in the pathogenesis of age-related macular degeneration. *Surv Ophthalmol*. 2000;45:115–134.
17. Bramall AN, Wright AF, Jacobson SG, McInnes RR. The genomic, biochemical, and cellular responses of the retina in inherited photoreceptor degenerations and prospects for the treatment of these disorders. *Annu Rev Neurosci*. 2010;33:441–472.
18. Plafker SM, O'Mealey GB, Szweda LI. Mechanisms for countering oxidative stress and damage in retinal pigment epithelium. *Int Rev Cell Mol Biol*. 2012;298:135–177.
19. Kang KH, Lemke G, Kim JW. The PI3K-PTEN tug-of-war, oxidative stress and retinal degeneration. *Trends Mol Med*. 2009;15:191–198.
20. Yu DY, Cringle SJ, Su EN, Yu PK. Intraretinal oxygen levels before and after photoreceptor loss in the RCS rat. *Invest Ophthalmol Vis Sci*. 2000;41:3999–4006.
21. Yu DY, Cringle S, Valter K, Walsh N, Lee D, Stone J. Photoreceptor death, trophic factor expression, retinal oxygen status, and photoreceptor function in the P23H rat. *Invest Ophthalmol Vis Sci*. 2004;45:2013–2019.

22. Komeima K, Rogers BS, Lu L, Campochiaro PA. Antioxidants reduce cone cell death in a model of retinitis pigmentosa. *Proc Natl Acad Sci U S A*. 2006;103:11300–11305.
23. Komeima K, Rogers BS, Campochiaro PA. Antioxidants slow photoreceptor cell death in mouse models of retinitis pigmentosa. *J Cell Physiol*. 2007;213:809–815.
24. Usui S, Oveson BC, Lee SY, et al. NADPH oxidase plays a central role in cone cell death in retinitis pigmentosa. *J Neurochem*. 2009;110:1028–1037.
25. Donovan M, Carmody RJ, Cotter TG. Light-induced photoreceptor apoptosis in vivo requires neuronal nitric-oxide synthase and guanylate cyclase activity and is caspase-3-independent. *J Biol Chem*. 2001;276:23000–23008.
26. Payne AJ, Kaja S, Naumchuk Y, Kunjukunju N, Koulen P. Antioxidant drug therapy approaches for neuroprotection in chronic diseases of the retina. *Int J Mol Sci*. 2014;15:1865–1886.
27. Cai X, McGinnis JF. Oxidative stress: the achilles' heel of neurodegenerative diseases of the retina. *Front Biosci (Landmark Ed)*. 2012;17:1976–1995.
28. Bedard K, Krause KH. The NOX family of ROS-generating NADPH oxidases: physiology and pathophysiology. *Physiol Rev*. 2007;87:245–313.
29. Thrasher AJ, Keep NH, Wientjes F, Segal AW. Chronic granulomatous disease. *Biochim Biophys Acta*. 1994;1227:1–24.
30. Bokoch GM, Zhao T. Regulation of the phagocyte NADPH oxidase by Rac GTPase. *Antioxid Redox Signal*. 2006;8:1533–1548.
31. Vignais PV. The superoxide-generating NADPH oxidase: structural aspects and activation mechanism. *Cell Mol Life Sci*. 2002;59:1428–1459.
32. Nauseef WM. Biological roles for the NOX family NADPH oxidases. *J Biol Chem*. 2008;283:16961–16965.
33. Takeya R, Sumimoto H. Regulation of novel superoxide-producing NAD(P)H oxidases. *Antioxid Redox Signal*. 2006;8:1523–1532.
34. Hordijk PL. Regulation of NADPH oxidases: the role of Rac proteins. *Circ Res*. 2006;98:453–462.
35. McCann SK, Roulston CL. NADPH oxidase as a therapeutic target for neuroprotection against ischaemic stroke: future perspectives. *Brain Sci*. 2013;3:561–598.
36. Lambeth JD. Nox enzymes, ROS, and chronic disease: an example of antagonistic pleiotropy. *Free Radic Biol Med*. 2007;43:332–347.
37. Hernandes MS, Britto LR. NADPH oxidase and neurodegeneration. *Curr Neuropharmacol*. 2012;10:321–327.
38. Nayernia Z, Jaquet V, Krause KH. New insights on NOX enzymes in the central nervous system. *Antioxid Redox Signal*. 2014;20:2815–2837.
39. Sarfstein R, Gorzalczany Y, Mizrahi A, et al. Dual role of Rac in the assembly of NADPH oxidase, tethering to the membrane and activation of p67phox: a study based on mutagenesis of p67phox-Rac1 chimeras. *J Biol Chem*. 2004;279:16007–16016.
40. Haruta M, Bush RA, Kjellstrom S, et al. Depleting Rac1 in mouse rod photoreceptors protects them from photo-oxidative stress without affecting their structure or function. *Proc Natl Acad Sci U S A*. 2009;106:9397–9402.
41. Li Q, Dinculescu A, Shan Z, et al. Downregulation of p22phox in retinal pigment epithelial cells inhibits choroidal neovascularization in mice. *Mol Ther*. 2008;16:1688–1694.
42. Dvoriantchikova G, Grant J, Santos AR, Hernandez E, Ivanov D. Neuronal NAD(P)H oxidases contribute to ROS production and mediate RGC death after ischemia. *Invest Ophthalmol Vis Sci*. 2012;53:2823–2830.
43. Bhatt L, Groeger G, McDermott K, Cotter TG. Rod and cone photoreceptor cells produce ROS in response to stress in a live retinal explant system. *Mol Vis*. 2010;16:283–293.
44. Jaffe AB, Hall A. Rho GTPases: biochemistry and biology. *Annu Rev Cell Dev Biol*. 2005;21:247–269.
45. Heasman SJ, Ridley AJ. Mammalian Rho GTPases: new insights into their functions from in vivo studies. *Nat Rev Mol Cell Biol*. 2008;9:690–701.
46. Diekmann D, Abo A, Johnston C, Segal AW, Hall A. Interaction of Rac with p67phox and regulation of phagocytic NADPH oxidase activity. *Science*. 1994;265:531–533.
47. Hassanain HH, Gregg D, Marcelo ML, et al. Hypertension caused by transgenic overexpression of Rac1. *Antioxid Redox Signal*. 2007;9:91–100.
48. Choi DH, Cristovao AC, Guhathakurta S, et al. NADPH oxidase 1-mediated oxidative stress leads to dopamine neuron death in Parkinson's disease. *Antioxid Redox Signal*. 2012;16:1033–1045.
49. Valencia A, Sapp E, Kimm JS, et al. Elevated NADPH oxidase activity contributes to oxidative stress and cell death in Huntington's disease. *Hum Mol Genet*. 2013;22:1112–1131.
50. Song H, Bush RA, Vijayasarathy C, Fariss RN, Kjellstrom S, Sieving PA. Transgenic expression of constitutively active RAC1 disrupts mouse rod morphogenesis. *Invest Ophthalmol Vis Sci*. 2014;55:2659–2668.
51. Park TK, Wu Z, Kjellstrom S, et al. Intravitreal delivery of AAV8 retinoschisin results in cell type-specific gene expression and retinal rescue in the Rs1-KO mouse. *Gene Ther*. 2009;16:916–926.
52. Miller FJ Jr, Griendling KK. Functional evaluation of non-phagocytic NAD(P)H oxidases. *Methods Enzymol*. 2002;353:220–233.
53. Jensen EC. Quantitative analysis of histological staining and fluorescence using ImageJ. *Anat Rec (Hoboken)*. 2013;296:378–381.
54. Wehr NB, Levine RL. Quantification of protein carbonylation. *Methods Mol Biol*. 2013;965:265–281.
55. Yagi K. Simple assay for the level of total lipid peroxides in serum or plasma. *Methods Mol Biol*. 1998;108:101–106.
56. Byrne LC, Dalkara D, Luna G, et al. Viral-mediated RdCVF and RdCVFL expression protects cone and rod photoreceptors in retinal degeneration. *J Clin Invest*. 2015;125:105–116.
57. Kawakami-Mori F, Shimosawa T, Mu S, et al. NADPH oxidase-mediated Rac1 GTP activity is necessary for nongenomic actions of the mineralocorticoid receptor in the CA1 region of the rat hippocampus. *Am J Physiol Endocrinol Metab*. 2012;302:E425–E432.
58. Bindokas VP, Jordan J, Lee CC, Miller RJ. Superoxide production in rat hippocampal neurons: selective imaging with hydroethidine. *J Neurosci*. 1996;16:1324–1336.
59. Dalle-Donne I, Rossi R, Giustarini D, Milzani A, Colombo R. Protein carbonyl groups as biomarkers of oxidative stress. *Clin Chim Acta*. 2003;329:23–38.
60. Esterbauer H, Schaur RJ, Zollner H. Chemistry and biochemistry of 4-hydroxynonenal, malonaldehyde and related aldehydes. *Free Radic Biol Med*. 1991;11:81–128.
61. Nielsen F, Mikkelsen BB, Nielsen JB, Andersen HR, Grandjean P. Plasma malondialdehyde as biomarker for oxidative stress: reference interval and effects of life-style factors. *Clin Chem*. 1997;43:1209–1214.
62. Cheng G, Diebold BA, Hughes Y, Lambeth JD. Nox1-dependent reactive oxygen generation is regulated by Rac1. *J Biol Chem*. 2006;281:17718–17726.
63. Belmonte MA, Santos MF, Kihara AH, Yan CY, Hamassaki DE. Light-induced photoreceptor degeneration in the mouse involves activation of the small GTPase Rac1. *Invest Ophthalmol Vis Sci*. 2006;47:1193–1200.

Investigative Ophthalmology & Visual Science

64. Roehlecke C, Schumann U, Ader M, et al. Stress reaction in outer segments of photoreceptors after blue light irradiation. *PLoS One*. 2013;8:e71570.
65. Chartier FJ, Hardy EJ, Laprise P. Crumbs limits oxidase-dependent signaling to maintain epithelial integrity and prevent photoreceptor cell death. *J Cell Biol*. 2012;198:991–998.
66. Saito Y, Uppal A, Byfield G, Budd S, Hartnett ME. Activated NAD(P)H oxidase from supplemental oxygen induces neovascularization independent of VEGF in retinopathy of prematurity model. *Invest Ophthalmol Vis Sci*. 2008;49:1591–1598.
67. Wilkinson-Berka JL, Rana I, Armani R, Agrotis A. Reactive oxygen species, Nox and angiotensin II in angiogenesis: implications for retinopathy. *Clin Sci (Lond)*. 2013;124:597–615.
68. Wilkinson-Berka JL, Deliyanti D, Rana I, et al. NADPH oxidase, NOX1, mediates vascular injury in ischemic retinopathy. *Antioxid Redox Signal*. 2014;20:2726–2740.
69. Wang H, Yang Z, Jiang Y, Hartnett ME. Endothelial NADPH oxidase 4 mediates vascular endothelial growth factor receptor 2-induced intravitreal neovascularization in a rat model of retinopathy of prematurity. *Mol Vis*. 2014;20:231–241.
70. Zeng H, Ding M, Chen XX, Lu Q. Microglial NADPH oxidase activation mediates rod cell death in the retinal degeneration in rd mice. *Neuroscience*. 2014;275:54–61.
71. Ardeljan D, Chan CC. Aging is not a disease: distinguishing age-related macular degeneration from aging. *Prog Retin Eye Res*. 2013;37:68–89.
72. Kowluru RA, Kowluru A, Veluthakal R, et al. TIAM1-RAC1 signalling axis-mediated activation of NADPH oxidase-2 initiates mitochondrial damage in the development of diabetic retinopathy. *Diabetologia*. 2014;57:1047–1056.
73. Kleniewska P, Piechota A, Skibska B, Goraca A. The NADPH oxidase family and its inhibitors. *Arch Immunol Ther Exp (Warsz)*. 2012;60:277–294.
74. Du Y, Veenstra A, Palczewski K, Kern TS. Photoreceptor cells are major contributors to diabetes-induced oxidative stress and local inflammation in the retina. *Proc Natl Acad Sci U S A*. 2013;110:16586–16591.
75. Du Y, Cramer M, Lee CA, et al. Adrenergic and serotonin receptors affect retinal superoxide generation in diabetic mice: relationship to capillary degeneration and permeability. *FASEB J*. 2015;29:2194–2204.
76. Heumuller S, Wind S, Barbosa-Sicard E, et al. Apocynin is not an inhibitor of vascular NADPH oxidases but an antioxidant. *Hypertension*. 2008;51:211–217.
77. Simons JM, Hart BA, Ip Vai Ching TR, Van Dijk H, Labadie RP. Metabolic activation of natural phenols into selective oxidative burst agonists by activated human neutrophils. *Free Radic Biol Med*. 1990;8:251–258.
78. Ding XQ, Quiambao AB, Fitzgerald JB, Cooper MJ, Conley SM, Naash MI. Ocular delivery of compacted DNA-nanoparticles does not elicit toxicity in the mouse retina. *PLoS One*. 2009;4:e7410.
79. Balasubramanian N, Slepak VZ. Light-mediated activation of Rac-1 in photoreceptor outer segments. *Curr Biol*. 2003;13:1306–1310.
80. Organisciak DT, Darrow RM, Barsalou L, Kutty RK, Wiggert B. Susceptibility to retinal light damage in transgenic rats with rhodopsin mutations. *Invest Ophthalmol Vis Sci*. 2003;44:486–492.

Investigative Ophthalmology & Visual Science